



Towards Robust and High-performance Operations of Wave Energy Converters: an Adaptive Tube-based Model Predictive Control Approach

DOI:

[10.1016/j.ifacol.2022.10.452](https://doi.org/10.1016/j.ifacol.2022.10.452)

Document Version

Accepted author manuscript

[Link to publication record in Manchester Research Explorer](#)

Citation for published version (APA):

Zhang, Y., & Li, G. (2022). Towards Robust and High-performance Operations of Wave Energy Converters: an Adaptive Tube-based Model Predictive Control Approach. *IFAC-PapersOnLine*, 55(31), 339-344. <https://doi.org/10.1016/j.ifacol.2022.10.452>

Published in:

IFAC-PapersOnLine

Citing this paper

Please note that where the full-text provided on Manchester Research Explorer is the Author Accepted Manuscript or Proof version this may differ from the final Published version. If citing, it is advised that you check and use the publisher's definitive version.

General rights

Copyright and moral rights for the publications made accessible in the Research Explorer are retained by the authors and/or other copyright owners and it is a condition of accessing publications that users recognise and abide by the legal requirements associated with these rights.

Takedown policy

If you believe that this document breaches copyright please refer to the University of Manchester's Takedown Procedures [<http://man.ac.uk/04Y6Bo>] or contact uml.scholarlycommunications@manchester.ac.uk providing relevant details, so we can investigate your claim.



Towards Robust and High-performance Operations of Wave Energy Converters: an Adaptive Tube-based Model Predictive Control Approach

Yujia Zhang* Guang Li**

* School of Engineering and Material Science, Queen Mary University of London (e-mail: yujia.zhang@qmul.ac.uk).

** School of Engineering and Material Science, Queen Mary University of London (e-mail: g.li@qmul.ac.uk)

Abstract: Model predictive control (MPC) is an effective control method to improve the energy conversion efficiency of wave energy converters (WECs). However, the current developed WEC MPC has not reached commercial viability since the control performance is significantly dependent on the WEC model fidelity. To overcome the plant-model mismatch issue in the WEC MPC control problem, this paper proposes a robust tube-based MPC method to bound plant states within disturbance invariant sets centered around the noise-free model trajectory. The invariant sets are also utilized for tightening the nominal model's constraints that robustly enable constraint satisfaction. Yet overly conservative invariant sets can narrow the feasible region of the states and control inputs, and hence a data-driven quantile recurrent neural network (QRNN) is proposed in this work to form a learning-based adaptive tube with reduced conservatism by quantifying WEC model uncertainties. The theoretical root is that time-dependent historical data can offer valuable insight into the future behaviour of uncertainties. Numerical simulations have validated that the proposed method can improve the energy capture rate compared to the TMPC approach, by synthesizing the QRNN-based tube with MPC.

Copyright © 2022 The Authors. This is an open access article under the CC BY-NC-ND license (<https://creativecommons.org/licenses/by-nc-nd/4.0/>)

Keywords: Control applications in marine renewable energy, Ocean renewable energy, Adaptive and robust control in marine systems

1. INTRODUCTION

Ocean waves contain tremendous clean and renewable energy, which have the potential to supply a great magnitude of electricity and help reduce the world's reliance on fossil fuels. Compared to other renewable sources such as solar and wind, wave power is more consistent and of higher density. Yet wave energy converters (WECs) have not been commercialized since harnessing irregular reciprocating wave motions is a challenging engineering problem. Control methods are thereby proposed to improve the economic return of WECs, e.g., latching control by adjusting the WEC frequency to wave frequencies (Budal et al. (1980)), impedance matching control by tuning dynamical parameters of the device (Babarit et al. (2009)), etc. The optimization-based model predictive control (MPC) strategy can improve wave energy conversion efficiency of these conventional methods and simultaneously maintain the safe operation of WECs (Li and Belmont (2014)). The controller can incorporate short-term wave predictions to further increase the extracted wave energy.

The performance of the established WEC MPC is dependent on WEC model fidelity. Less complicated and sufficiently accurate models are preferable in the control scheme. However, disturbances inevitably exist in real-world scenarios that contribute to WEC model uncertainties, e.g., imprecise estimations of WEC

hydrodynamic parameters, wave prediction errors. The usage of the exact same WEC model for control design and performance evaluation hence may obtain misleading results. In this context, various strategies have recently been developed to enhance the robustness of WEC MPC, such as (i) pre-stabilized feedback robust MPC (RMPC) of WEC (Zhan et al. (2019b)), which utilizes an unconstrained optimization to maximize the nominal system's energy output and applies a feedback portion to cope with uncertainties; (ii) Laguerre-polynomial-based robust WEC MPC, which augments the standard MPC with feedback and adopts the Laguerre polynomial to alleviate the computational burden (Jama et al. (2018)). A powerful alternative is the robust tube-based MPC (TMPC) law that explicitly deals with uncertainties by bounding possible disturbances in a bundle/tube of disturbance invariant sets centered around the nominal system trajectory. Here the invariant sets are defined as the tube cross-sections. Accordingly, constraint satisfaction for the uncertain states can be guaranteed by tightening system constraints with the tube. Note that the tube is constructed offline without influencing the online computational complexity.

However, the tube employed in the traditional TMPC algorithm might be overly conservative that narrows the feasible region of the states and control inputs. When a constraint is active or near-saturated, shrinking the tube cross-section by uncertainty parameterization at each sampling time can provide a larger feasible set to improve WEC control performance. Inspired by the reality that time-dependent historical data can offer valuable insight into future uncertainty and capture the distribution of the uncertain dynamics, a data-driven adaptive tube MPC is de-

* The authors acknowledge the support of Wave Energy Control Systems Programme in part by Innovate UK Energy Catalyst Round 8 project: Sea Wave Energy Powered Microgrid for Remote Islands and Rural Coasts (No. 86116), and in part by EPSRC projects with grant numbers EP/P023002/1.

veloped to bound the tail of uncertainty distribution (Fan et al. (2020)) and therefore reduce the conservatism of conventional general inclusive invariant sets. The tube of WEC uncertainties is computed by the quantile recurrent neural network (QRNN), which utilizes a long short-term memory (LSTM) (Hochreiter and Schmidhuber (1997)) type recurrent neural network (RNN) (Yu et al. (2019)) trained with a quantile-regression-based loss function (Yu et al. (2003)). Employment of the quantile loss is to compute the uncertain trajectories' probabilistic bounds; adopting a relative high quantile can bound the majority of uncertain WEC states. In addition, the utilization of LSTM is attributed to its excellent performance in dealing with time-series data, since the WECs' uncertainty is a chronological sequence. Therefore, robust and high-performance operations of WEC systems can be achieved by synthesizing the QRNN-based tube into the TMPC; online tractability of the WEC control problem can be ensured as the network training is implemented offline.

The rest of the paper is organized as follows: Section 2 presents the WEC modeling problem and the corresponding control objective. In Section 3, the LT MPC approach tailored for WECs is discussed. Numerical simulation results are provided in Section 4, and the concluding remarks are summarized in Section 5.

2. PROBLEM SET-UP AND PRELIMINARIES

A point-absorber type WEC device for wave energy extraction studied in this work is shown in Fig. 1, where a buoy floats on the sea surface and an upright standing hydraulic cylinder is fixed to a gravity base attached to the seabed. The heave motions of the buoy generate relative movements between a piston and a hydraulic cylinder. Consequently, a liquid flow is generated by the relative motions. The flow drives the generator-connected hydraulic motors of a power take-off (PTO) device to convert wave energy into electricity through AC/DC/AC converters. Control of the energy conversion process involves exerting a manipulative force f_u on the PTO system to manage the generator-side electric torque. The extracted power is $P = -f_u v$, where v is the velocity on the piston.

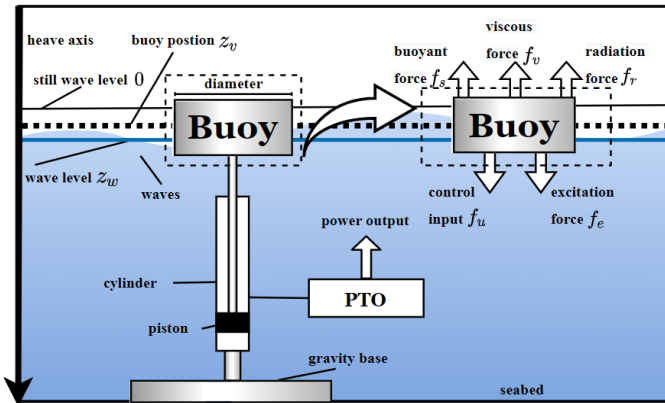


Fig. 1. Schematic diagram of the point absorber

Following the Newtonian mechanics, the dynamic model of the buoy is formulated in (1).

$$m_s \ddot{z}_v(t) = -f_r(t) + f_e(t) - f_s(t) - f_v(t) + f_u(t) \quad (1)$$

where f_u is the exerted force on the piston as the control input. f_r denotes the radiation force (Torr (1984)). f_e is the excitation force (Nguyen and Tona (2017)) introduced by incident waves. f_s and f_v represent the buoyant force (Jean and Fan (1992))

and viscous force (Wei et al. (2015)), respectively. Besides, we employ the parameter m_s to denote the buoy mass and z_v to denote the position of the floating buoy's middle point such that $v = \dot{z}_v$.

The radiation force $f_r(t)$ is given by

$$f_r(t) = m_\infty \ddot{z}_v(t) + \int_{-\infty}^{\infty} h_r(\tau) \dot{z}_v(t - \tau) d\tau \quad (2)$$

Here m_∞ is the added mass on the float. h_r denotes the kernel of the radiation force that can be calculated by hydraulic software such as WAMIT (Lee and Newman (2001)). The convolutional term in (2) can be expressed through a state-space model with an order of n_r (Yu and Falnes (1995)).

$$\dot{x}_r(t) = A_r x_r(t) + B_r \dot{z}_v(t) \quad (3a)$$

$$f_r(t) = C_r x_r(t) \approx \int_{-\infty}^t h_r(\tau) \dot{z}_v(t - \tau) d\tau \approx f_r(t) - m_\infty \ddot{z}_v(t) \quad (3b)$$

in which $x_r \in \mathbb{R}^{n_r}$, and $(A_r, B_r, C_r, 0)$ denote its state-space realization. Besides, the wave excitation force f_e is calculated in (5) following the work proposed by Yu and Falnes (1995).

$$f_e(t) = \int_{-\infty}^{\infty} h_e(\tau) z_w(t - \tau) d\tau \quad (4)$$

$$\dot{x}_e(t) = A_e x_e(t) + B_e z_w(t) \quad (5a)$$

$$f_e(t) = C_e x_e(t) \approx \int_{-\infty}^t h_e(\tau) z_w(t - \tau) d\tau \quad (5b)$$

The state-space expression of f_e relies on the excitation kernel h_e . x_e and $(A_e, B_e, C_e, 0)$ are the corresponding intermediate state and the state-space realization.

In addition, the buoyancy is expressed as

$$f_s(t) = \rho g S z_v(t) \quad (6)$$

where ρ is water density. g denotes the standard gravity, and S denotes the cross-sectional area of the float. If a hydrostatic stiffness $k_s := \rho g S$ is introduced, the buoyancy is given by $f_s(t) = k_s z_v(t)$.

The nonlinear viscous forces also exert on the buoy, and the viscous force is formulated as (7), where C_d represents the drag coefficient (Giorgi and Ringwood (2017)).

$$f_v(t) = \frac{1}{2} \rho C_d S |\dot{z}_v(t)| \dot{z}_v(t) \quad (7)$$

The forces mentioned above altogether lead to the state-space realization of the buoy's dynamic model, given by

$$\dot{x}_c(t) = A_c x_c(t) + B_{uc} u_c(t) + B_{wc} z_w(t) + \epsilon(t) \quad (8a)$$

$$z(t) = C_z x_c(t) \quad (8b)$$

where (A_c, B_{uc}, B_{wc}) denote the continuous-time state-space expression of the forces on the floating buoy formulated in (9). The output z is the heave velocity \dot{z}_v and C_z is the output matrix. ϵ represents the modeling errors from the approximations of radiation and excitation forces. In addition, the state of the WEC model is chosen as $x_c = [z_v, \dot{z}_v, x_r, x_e]^T$ with an order of n , and the control input as $u_c = f_u$. The state and control are bounded within compact constraint sets \mathbb{X} and \mathbb{U} , respectively.

$$A_c = \begin{bmatrix} 0 & 1 & 0_{1 \times n_r} & 0_{1 \times n_e} \\ -k_s/m - \frac{1}{2} \rho C_d S |\dot{z}_v|/m - C_r/m & C_e/m & A_r & 0_{n_r \times n_e} \\ 0_{n_r \times 1} & B_r & A_r & 0_{n_r \times n_e} \\ 0_{n_e \times 1} & 0_{n_e \times 1} & 0_{n_e \times n_r} & A_e \end{bmatrix}, \quad B_{uc} = \begin{bmatrix} 0 \\ 1/m \\ 0_{n_r \times 1} \\ 0_{n_e \times 1} \end{bmatrix}$$

$$B_{wc} = [0, 0, 0_{n_r \times 1}, B_c]^T, C_z = [0, 1, 0_{1 \times (n_r + n_e)}] \quad (9)$$

In the above expressions, m equals the sum of the buoy mass m_s and added mass m_∞ . Due to the presence of nonlinear hydrodynamics in A_c of (9), the constructed model in (8) describes a nonlinear WEC system, which may be intractable for online computation. Hence a linear WEC model \bar{f} is utilized to approximate the intrinsically nonlinear WEC since the system has only mild nonlinearity. The linear model \bar{f} is derived with discretization and linearization of (8), and is supposed to be a noise-free nominal model denoted by

$$\bar{x}^+ = \bar{f}(x) = A\bar{x} + B_u\bar{u} + B_w z_w \quad (10a)$$

$$\bar{z} = C_z \bar{x} \quad (10b)$$

where \bar{x} and \bar{u} denote the nominal state and input in the current time. \bar{x}^+ is the successor state of \bar{x} , and \bar{z}_v is the nominal output. $[A, B_u, B_w]$ are derived from the local linearization of (8) using the Jacobian matrix.

In comparison, a sampled-data system of the nonlinear dynamics (8) is defined as the uncertain model to approximate the disturbed WEC system, and its dynamics is

$$x^+ = f(x) = Ax + B_u u + B_w z_w + w(x, u) \quad (11a)$$

$$z = C_z x \quad (11b)$$

The above denotation w includes (i) the model uncertainties from inaccurate radiation and excitation force approximations when establishing their state-space models (8); (ii) the model mismatches brought by the local linearization; (iii) errors in estimating parameters such as the drag coefficient. w is assumed to be bounded that $w \in \mathbb{W} \subseteq \mathbb{X}$.

3. LEARNING-BASED TUBE MPC FORMULATION FOR THE WEC CONTROL PROBLEM

3.1 Conventional tube MPC formulation for WECs

In this section, a robust TMPC strategy is developed according to the WEC state-space model to maximize wave energy extraction. The formulated control problem adopts an energy-maximization objective function to optimize the nominal model trajectories, and the uncertain trajectories are bounded around the nominal states in a tube of disturbance invariant sets. The boundedness essentially implies the controller's inherent robustness as the TMPC always steers the uncertain trajectories close to nominal.

Disturbance invariant set for uncertainty handling: To investigate the disturbance invariant set mentioned above, the model discrepancy between the nominal state \bar{x} and the uncertain state x is first studied. The discrepancy is denoted as e , and its evolution can be formulated as

$$e_{k+1} = Ae_k + B_u(u_k - \bar{u}_k) + w_k \quad (12)$$

If e is penalized with a feedback component κ to construct a feedback controller u in the form of $u = \bar{u} + \kappa(x - \bar{x}) = \bar{u} + \kappa e$, the evolutionary trajectory of e_k is

$$e_k = A^k e_0 + \sum_{j=0}^{k-1} A^{k-j-1} B_u (u_j - \bar{u}_j) + \sum_{j=0}^{k-1} A^{k-j-1} w_j \quad (13)$$

Denote $A_k \triangleq A + B_u \kappa$. Since $u = \bar{u} + \kappa e$ and $w \in \mathbb{W}$, the set \mathcal{E} that contains all possible uncertainties should yield $\mathcal{E}_k \triangleq$

$A_k^{k-1} \mathbb{W} \oplus A_k^{k-2} \mathbb{W} \oplus \dots \oplus A_k \mathbb{W} \oplus \mathbb{W}$ at time $k \in \mathbb{N}_+$. \mathcal{E}_k bounds all uncertainties in a tube to guarantee $x_k = \bar{x}_k \oplus \mathcal{E}_k$ and $u_k \in \bar{u}_k \oplus \kappa \mathcal{E}_k$, where the tube centers in the nominal trajectories \bar{x} and \bar{u} (Mayne et al. (2005)). If $k \rightarrow \infty$, a rigid disturbance invariant set \mathcal{E} can be computed to bound all possible uncertainties, such that $\mathcal{E} = \sum_{i=0}^{\infty} A_k^i \mathbb{W}$ (Σ denotes the set addition). Given that A_k is Schur stable, the set \mathcal{E} has the form $A_k \mathcal{E} \oplus \mathbb{W} \in \mathcal{E}$.

By assuming $\text{pre}(\mathcal{E})$ is the pre-set of \mathcal{E} that evolves into the target set \mathcal{E} in one step, the above statement equals to guaranteeing $\mathcal{E} \subseteq \text{pre}(\mathcal{E})$ or $\mathcal{E} \cap \text{pre}(\mathcal{E}) = \mathcal{E}$ considering $A_k \mathcal{E} \oplus \mathbb{W}$ is the posterior set of \mathcal{E} (Zeilinger et al. (2014)). If there exists a finite k to satisfy the above condition, the computation of \mathcal{E} can be simplified into a set addition in finite time. But in practice, we adopt a finite set addition $\mathcal{E}_j = \sum_{i=0}^j A_k^i \mathbb{W}$ to approximate \mathcal{E} even if $\mathcal{E} \subseteq \text{pre}(\mathcal{E})$ cannot be achieved in finite time.

With the determined \mathcal{E} , given that the uncertain state trajectories, control inputs and disturbances are subject to the polyhedral constraint sets $(\mathbb{X}, \mathbb{U}, \mathbb{W}) \triangleq \{x \in \mathbb{R}^n, u \in \mathbb{R}^m, w \in \mathbb{R}^n | Fx \leq g, Hu \leq i, Jw \leq q\}$, all nominal constraint sets need to be tightened with \mathcal{E} to guarantee the disturbed states maintained within \mathbb{X} and \mathbb{U} , since $\bar{x} \oplus \mathcal{E} \subseteq \mathbb{X}$ and $\bar{u} \oplus \kappa \mathcal{E} \subseteq \mathbb{U}$. If the tightened nominal state set is denoted as $\bar{\mathbb{X}}$ and the tightened nominal control set is $\bar{\mathbb{U}}$, it can be deduced that $\bar{\mathbb{X}} \triangleq \mathbb{X} \ominus \mathcal{E}$ and $\bar{\mathbb{U}} \triangleq \mathbb{U} \ominus \kappa \mathcal{E}$, where $(\bar{\mathbb{X}}, \bar{\mathbb{U}}) \triangleq \{\bar{x} \in \mathbb{R}^n, \bar{u} \in \mathbb{R}^m | \bar{F}\bar{x} \leq \bar{g}, \bar{H}\bar{u} \leq \bar{i}\}$. The inequalities represent a set projection of the polyhedra constraints onto each state, denoted as Projection $_{\bar{x}_i}(\bar{\mathbb{X}})$, where $\bar{x}_i \in \mathbb{R}$ is a projected state to enable Projection $_{\bar{x}_i}(\bar{\mathbb{X}}) = \{\forall \bar{x}_i \in \mathbb{R}, \exists \bar{y} \in \mathbb{R}^n \text{ such that } (\bar{x}, \bar{y}) \in \bar{\mathbb{X}}\}$.

Tube MPC: Following the above uncertainty handling method, we can determine the nominal control \bar{u} and state \bar{x} by solving a constrained optimization problem. The formulated objective can extract the maximum time average energy based on the nominal model and enable the safety of operations. Assume the prediction horizon is N , and the simulation horizon is H_t . The optimization problem is given as

$$V_N(\bar{x}, \bar{u}) = \min_u \sum_{k=0}^{N-1} \left(\frac{1}{2} \|\bar{x}(k)\|_Q^2 + \bar{z}(k) \bar{u}(k) + \frac{1}{2} \|\bar{u}(k)\|_R^2 \right) \quad (14)$$

$$\text{s.t. } \bar{x}(k+1) = A\bar{x}(k) + B_u \bar{u}(k) + B_w z_w(k) \quad (14a)$$

$$\bar{z}(k) = C_z \bar{x}(k) \quad (14b)$$

$$\bar{x}(k) + \mathcal{E} \in \mathbb{X}, \forall \bar{x}(k) \in \bar{\mathbb{X}} \subseteq \mathbb{X} \quad (14c)$$

$$\bar{u}(k) + \kappa \mathcal{E} \in \mathbb{U}, \forall \bar{u}(k) \in \bar{\mathbb{U}} \subseteq \mathbb{U} \quad (14d)$$

$$x(k+1) = Ax(k) + B_u u(k) + B_w z_w(k) + w(k), \quad (14e)$$

$$\forall x(k) \in \mathbb{X}, \forall u(k) \in \mathbb{U}, \forall w(k) \in \mathbb{W} \quad (14e)$$

$$\mathbb{X} = \bar{\mathbb{X}} \oplus \mathcal{E}, \mathbb{U} = \bar{\mathbb{U}} \oplus \kappa \mathcal{E} \quad (14f)$$

The minimization of the term $\bar{z}\bar{u}$ is equivalent to the maximization of the captured power $P_k = -f_u(k) \dot{z}_v(k)$. In practice, the economic return requires to be maximized for guaranteeing a high level of energy conversion efficiency and decrease the consumed energy by actuators. We therefore penalize the consumed energy in the control objective (14) such that $\|\bar{u}(k)\|_R^2$. Penalization of the term $\|\bar{x}(k)\|_Q^2$ enables the convexity of the objective (14) and reduces risks of device damage brought by stringent state responses (Li and Belmont (2014)). Note that the

feasibility of (14) can be proved through imposing an invariant set tightened by \mathcal{E} to bound the terminal nominal states (Zhan et al. (2019b)), where all state sequences will evolve into the invariant set (Mayne et al. (2005)). Moreover, the input-to-state stability method for stability analysis employed by this type of MPC has been investigated in our recent WEC MPC control work (Zhan et al. (2019a), Zhan et al. (2019b)), and can be further extended for the robust stability analysis of the learning-based TMPC. The proofs are omitted here due to the page limitation.

To obtain the solution of the control problem, (14) can be formulated into a standard QP form, where (14a) is rewritten as

$$\hat{X} = \hat{A}\hat{x}_{k|0} + \hat{B}_u\hat{U} + \hat{B}_w\hat{Z}_w \quad (15)$$

Here $\hat{X} = [\hat{x}_{k|0} \ \hat{x}_{k|1} \ \dots \ \hat{x}_{k|N-1}]^T$, $\hat{U} = [\hat{u}_{k|0} \ \hat{u}_{k|1} \ \dots \ \hat{u}_{k|N-1}]^T$, $\hat{Z}_w = [z_{w(k|0)} \ z_{w(k|1)} \ \dots \ z_{w(k|N-1)}]^T$. And the objective (14) is reformulated as

$$V_N(\bar{x}, \bar{u}) = \frac{1}{2}\hat{X}^T\hat{Q}\hat{X} + \hat{U}^T\hat{C}_z\hat{X} + \frac{1}{2}\hat{U}^T\hat{R}\hat{U} \quad (16)$$

By substituting (15) into (16), the objective (14) yields

$$V_N(\bar{x}, \bar{u}) = \frac{1}{2}\hat{U}^T H \hat{U} + f^T \hat{U} + \beta \quad (17)$$

$$H = \hat{R} + \hat{B}_u^T \hat{Q} \hat{B}_u + 2\hat{B}_u^T \hat{C}_z^T \quad (17a)$$

$$f = (\hat{B}_u^T \hat{Q} + \hat{C}_z)(\hat{A}\hat{x}_{k|0} + \hat{B}_w\hat{Z}_w) \quad (17b)$$

$$\beta = \frac{1}{2}(\hat{A}\hat{x}_{k|0} + \hat{B}_w\hat{Z}_w)^T Q (\hat{A}\hat{x}_{k|0} + \hat{B}_w\hat{Z}_w) \quad (17c)$$

Note that though the solution of \hat{U} in (17) yields a control sequences $[\hat{u}_{k|0} \ \hat{u}_{k|1} \ \dots \ \hat{u}_{k|N-1}]^T$, only the first input $\{\hat{u}_{k|0} \mid \hat{u}_{k|0} \triangleq \bar{u}(0)\}$ is applied to the plant at each time.

To enhance the robustness, a feedback portion on the basis of the nominal control \bar{u} is applied.

$$u_{k|0} = \kappa(x_{k|0} - \bar{x}_{k|0}) + \bar{u}_{k|0} \quad (18)$$

where $\bar{u}_{k|0}$ denotes the nominal control in the optimal input sequence $[\bar{u}_{k|0}, \bar{u}_{k|1}, \dots, \bar{u}_{k|N-1}]$ solved from (14) using QP reformulation. κ denotes a feedback coefficient penalizing the error e . Hence the term $\kappa(x_{k|0} - \bar{x}_{k|0})$ enhances robustness of the nominal controller \bar{u} , which improves the wave energy conversion efficiency. The choice of κ should guarantee that all eigenvalues of A_k are strictly inside the unit circle.

From the above discussion, we can summarize the conventional tube-based MPC law as a synthesis of the tightened nominal MPC (TNMPC) and the feedback. The feedback portion has the potential to improve the wave energy extraction efficiency of the conventional MPC with model uncertainties present. Yet if the nominal constraints are active or near-saturated, the constraints might be overly tightened by the tube, which is not time or spacing varying that fails to capture the distribution of uncertainties. To address this issue, the set-addition-based rigid tube can be parameterized to be time-varying by utilizing machine learning techniques. The method essentially shrinks the tube cross-sections and provides a larger feasible set to make WEC constraints less inclined to be saturated.

3.2 QRNN-based tube parameterization

As the WEC state data contains valuable information of future uncertainties, the pattern of WEC uncertainty distribution can

be learned via training an data-driven neural network (NN) model. Here the NN input associates with a sequence of historical measurement data, including the wave predictions \bar{w} and ground truth data of the wave profile w , chronological inputs (\bar{u}, u) and WEC states (\bar{x}, x) . The output is a quantile description of the parameterized model mismatch f_e to bound the tail of f_e distribution since the construction of a tube is safety-critical. Denote f_e as

$$f_e(x) = \max\{\|x_i - \bar{x}_i\| / \text{Projection}_{x_i}(\mathcal{E}), i \in n\} \quad (19)$$

where $\text{Projection}_{x_i}(\mathcal{E})$ is the projection of the rigid disturbance invariant set \mathcal{E} onto a specific state x_i . $(x_i - \bar{x}_i)$ is the WEC plant-model mismatch for a certain state.

The NN output is assumed to be α -th probabilistic quantile bound of the resulting parameterized WEC model mismatches f_e . If the NN output is denoted as μ_α ($\mu_\alpha \in \mathbb{Y}$), and the input is $I = \{\bar{w}, w, \bar{u}, u, \bar{x}, x\}$, selection of α determines the conservativeness of the probabilistic tube bound, such that

$$\alpha = P(\mathbb{Y} \leq \mu_\alpha(I)) \equiv f_{\mathbb{Y}}(\mu_\alpha) \quad (20)$$

where P stands for probability. Note that (20) can be satisfied by training a quantile neural network which provides a probabilistic bound of f_e . The network adopts a check loss function (21) following Koenker and Bassett Jr (1978).

$$L^\alpha(f_e(x), \mu_\alpha(x)) = \begin{cases} \alpha(f_e(x) - \mu_\alpha(x)) & f_e(x) > \mu_\alpha(x) \\ (1 - \alpha)(\mu_\alpha(x) - f_e(x)) & f_e(x) \leq \mu_\alpha(x) \end{cases} \quad (21)$$

Here the utilized network is the long short-term memory (LSTM) network considering that LSTM has shown excellent performance in analyzing the patterns in chronological sequences. The training process starts from transforming the LSTM input data into a sequential internal state and is later deciphered to return a chronological sequence of future WEC uncertainty prediction. The prediction is compared with μ_α and their discrepancy is utilized for back-propagation to update the NN weights, where the check loss (21) is adopted for back-propagation. Then the trained network is synthesized into the conventional TMPC approach to propagate the WEC uncertainties forward with the learned dynamics model. We name the model as quantile LSTM (Q-LSTM), given that a quantile probabilistic output is integrated into LSTM to parameterize uncertainty distribution. To illustrate, a sequence of uncertain data is shown in blue dots in Fig. 2 for testing the accuracy of the trained neural network, 0.1, 0.5, 0.9 represents $\alpha = 10\%$, $\alpha = 50\%$, and $\alpha = 90\%$ respectively ($\alpha \in (0, 1)$), to parameterize a quantile probabilistic bound for uncertainties.

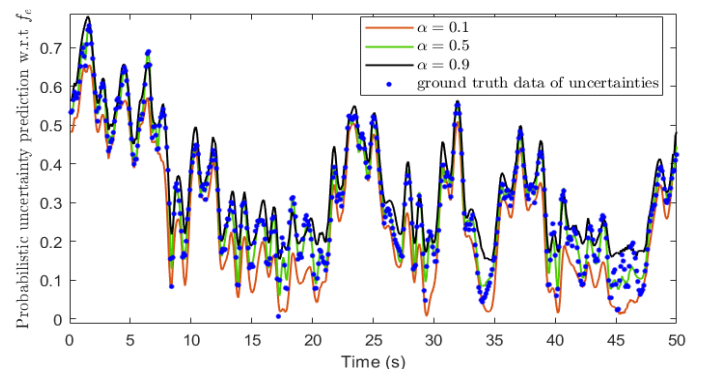


Fig. 2. Estimating quantile uncertainties with Q-LSTM

4. NUMERICAL RESULTS AND DISCUSSION

A set of wave predictions using the joint north sea wave project (JONSWAP) spectrum (Hasselmann et al. (1973)) is shown in Fig. 3 to demonstrate the efficacy of the proposed controller. Sources of uncertainties utilized in this system include (i) the model mismatch between the nominal model and the uncertain model caused by local linearization; (ii) the inaccurate modeling of radiation and excitation forces; (iii) the inaccurate estimation of the drag coefficient. Besides, we assume the control input subject to the constraint $\mathbb{U} = \{u \in \mathbb{R} \mid -2.5 \times 10^3 \leq u \leq 2.5 \times 10^3\}$, which are the main constraints in this problem. The uncertain state is restricted by $\mathbb{X} = \{x \in \mathbb{R}^n \mid [-2; -3; -\text{Inf}_{(n_r+n_e) \times 1}] \leq x \leq [2; 3; \text{Inf}_{(n_r+n_e) \times 1}]\}$.

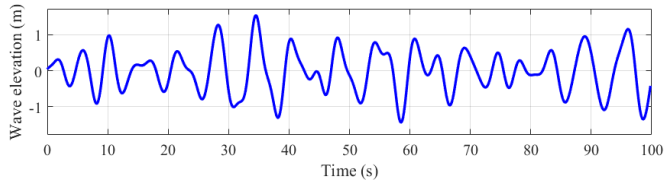


Fig. 3. 100-s period of wave profile in simulation.

The performance of the proposed learning-based tube MPC (LTMPC) is compared with conventional TMPC, nominal MPC and a well-tuned passive damper $u = K\dot{z}_v$. The passive damper is employed as a baseline controller for comparison purpose. By the trim of its input, the control constraints are enforced not to be violated. The nominal MPC is computed following a similar implementation process of TMPC, but no error feedback is applied and no constraint set is tightened. Both the conventional TMPC and LTMPC employ the same control parameters Q , R and the feedback coefficient κ , determined offline based on the nominal model. Here Q is chosen as $0_{n \times n}$ and R is 4×10^{-4} . κ is designed as $[-6.5 \times 10^3 \ -2 \times 10^2 \ 0_{1 \times (n_r+n_e)}]$ to counteract the plant-model mismatches. The constraint sets of conventional TMPC are tightened with the tube constructed from set addition while the tube for LTMPC is parameterized by QRNN. Note that the state trajectories with both LTMPC and conventional TMPC are required to evolve around the tightened nominal MPC (TNMPC) trajectory and stay within the computed tube.

Fig. 4~Fig. 6 show the input, heave position, heave velocity of the LTMPC (blue line), conventional TMPC (magenta line), TNMPC (red line), and the passive damper (green line). The states and controls of the LTMPC, TMPC and the passive damper should be bounded by the exerted constraints (black lines) to avoid potential WEC device damages. The trajectories with TNMPC should be restricted by the tightened nominal constraints $\bar{\mathbb{X}}$ and $\bar{\mathbb{U}}$ (grey lines) to impose a safe margin for disturbance evolutions as stated in Section 3. From the figures, the input constraints are active for all mentioned controllers since these inputs are observed to be saturated at different times, and the state constraints remain inactive over time. The saturation of inputs implies a fair comparison between the performance of these controllers. Besides, we especially note that, by proposing a QRNN-based uncertainty set utilizing $\alpha = 0.9$, the LTMPC can roughly satisfy the constraint sets such that $u \in \bar{\mathbb{U}} \oplus \kappa\mu_\alpha$ and $x \in \bar{\mathbb{X}} \oplus \mu_\alpha$ as shown in Fig. 4~Fig. 6, where $\kappa\mu_\alpha$ and μ_α are robust disturbance sets centered in TNMPC trajectories.

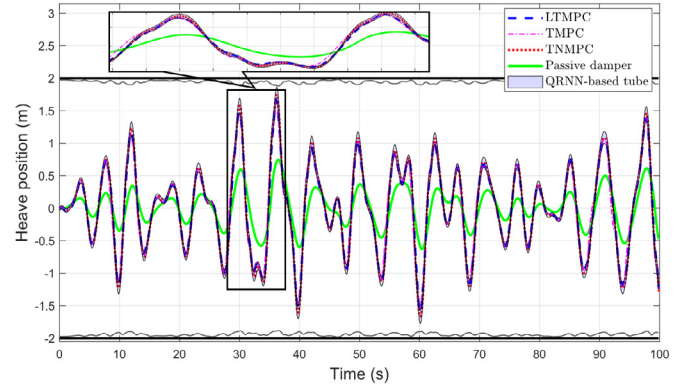


Fig. 5. Heave positions with different controllers

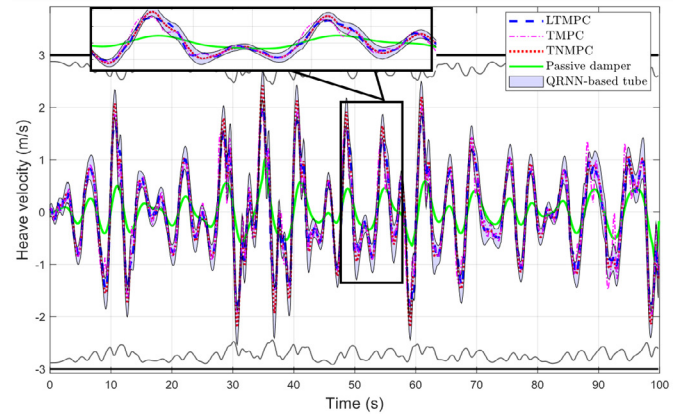


Fig. 6. Heave velocities with different controllers

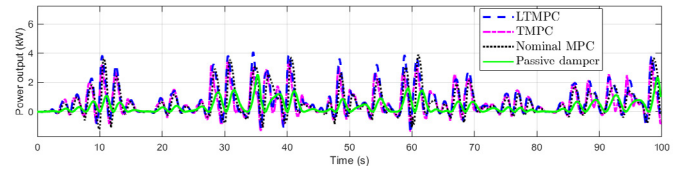


Fig. 7. Extracted wave power with LTMPC, TMPC, nominal MPC, and passive damper.

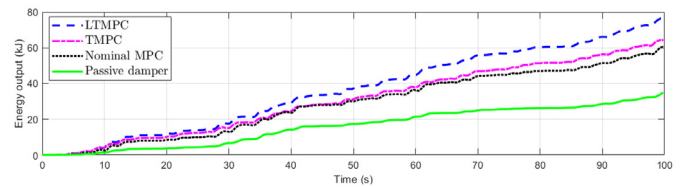


Fig. 8. Extracted wave energy with LTMPC, TMPC, nominal MPC, and passive damper.

Fig. 7 and Fig. 8 show the power and energy outputs with the LTMPC, conventional TMPC, the Nominal MPC (dotted black line), and the passive damper with the existence of model uncertainties. Compared with MPC methods, the passive damper captures less wave energy considering it is a non-optimization-based control method. The nominal MPC outperforms the passive damper but has not converted as much wave energy as TMPC controllers, given that the nominal controller is heavily dependent on the WEC fidelity and the model mismatch issue

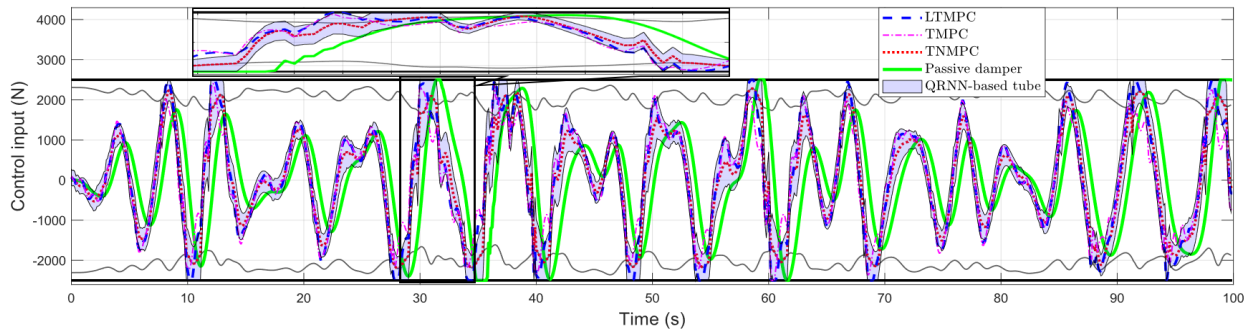


Fig. 4. Control inputs for the LTMPC, tightened nominal MPC, nominal MPC and passive damper. Input constraints are active.

in this case degrades its overall performance. In contrast, the TMPC is less susceptible to model uncertainties for its intrinsic robustness brought by the error feedback portion, and hence the energy extraction efficiency is observed to be improved. By applying the quantile learning technique to synthesize a more aggressive tube into TMPC, the proposed LTMPC strategy can extract more energy as the feasible region of the WEC control problem is enlarged compared with the conventional TMPC. From the perspective of computational performance, given that we determine the rigid tube and pre-train the QRNN offline, the online computation of LTMPC is enabled since its complexity approximately equals that of the conventional MPC.

5. CONCLUSION

In this paper, a control strategy based on LTMPC is developed for the point absorber type WEC device to improve the captured wave energy. The proposed controller parameterizes WEC uncertainties with QRNN, where the tail of the uncertainty distribution has been bounded so as to reduce the tube conservatism in the conventional TMPC. Besides, the real-time tractability of the proposed algorithm is guaranteed by training the QRNN offline. In our future work, we will attempt to enable the adaptability of the proposed LTMPC by including the change of sea states in the investigated uncertainties.

REFERENCES

- Babarit, A., Guglielmi, M., and Clément, A.H. (2009). De-clutching control of a wave energy converter. *Ocean engineering*, 36(12-13), 1015–1024.
- Budal, K. et al. (1980). Interacting point absorbers with controlled motion.
- Fan, D., Agha, A., and Theodorou, E. (2020). Deep learning tubes for tube mpc. doi:10.15607/RSS.2020.XVI.087.
- Giorgi, G. and Ringwood, J. (2017). Consistency of viscous drag identification tests for wave energy applications. In *Proceedings of the 12th European Wave and Tidal Energy Conference 27th Aug-1st Sept 2017*, 643, 1–8. European Wave and Tidal Energy Conference 2017.
- Hasselmann, K.F., Barnett, T.P., Bouws, E., Carlson, H., Cartwright, D.E., Eake, K., Euring, J., Gicnapp, A., Hasselmann, D., Kruseman, P., et al. (1973). Measurements of wind-wave growth and swell decay during the joint north sea wave project (jonswap). *Ergaenzungsheft zur Deutschen Hydrographischen Zeitschrift, Reihe A*.
- Hochreiter, S. and Schmidhuber, J. (1997). Long short-term memory. *Neural computation*, 9(8), 1735–1780.
- Jama, M., Wahyudie, A., and Noura, H. (2018). Robust predictive control for heaving wave energy converters. *Control Engineering Practice*, 77, 138–149.
- Jean, R.H. and Fan, L.S. (1992). On the model equations of gibilaro and focolo with corrected buoyancy force. *Powder technology*, 72(3), 201–205.
- Koenker, R. and Bassett Jr, G. (1978). Regression quantiles. *Econometrica: journal of the Econometric Society*, 33–50.
- Lee, C. and Newman, J. (2001). Solution of radiation problems with exact geometry. In *Proc. 16th Intl. Workshop on Water Waves and Floating Bodies. Hiroshima, Japan*, 93–96.
- Li, G. and Belmont, M.R. (2014). Model predictive control of sea wave energy converters—part i: A convex approach for the case of a single device. *Renewable Energy*, 69, 453–463.
- Mayne, D.Q., Seron, M.M., and Raković, S. (2005). Robust model predictive control of constrained linear systems with bounded disturbances. *Automatica*, 41(2), 219–224.
- Nguyen, H.N. and Tona, P. (2017). Wave excitation force estimation for wave energy converters of the point-absorber type. *IEEE Transactions on Control Systems Technology*, 26(6), 2173–2181.
- Torr, G. (1984). The acoustic radiation force. *American Journal of Physics*, 52(5), 402–408.
- Wei, Y., Rafiee, A., Henry, A., and Dias, F. (2015). Wave interaction with an oscillating wave surge converter, part i: Viscous effects. *Ocean Engineering*, 104, 185–203.
- Yu, K., Lu, Z., and Stander, J. (2003). Quantile regression: applications and current research areas. *Journal of the Royal Statistical Society: Series D (The Statistician)*, 52(3), 331–350.
- Yu, Y., Si, X., Hu, C., and Zhang, J. (2019). A review of recurrent neural networks: Lstm cells and network architectures. *Neural computation*, 31(7), 1235–1270.
- Yu, Z. and Falnes, J. (1995). State-space modelling of a vertical cylinder in heave. *Applied Ocean Research*, 17(5), 265–275.
- Zeilinger, M.N., Morari, M., and Jones, C.N. (2014). Soft constrained model predictive control with robust stability guarantees. *IEEE Transactions on Automatic Control*, 59(5), 1190–1202.
- Zhan, S., Li, G., and Bailey, C. (2019a). Economic feedback model predictive control of wave energy converters. *IEEE Transactions on Industrial Electronics*, 67(5), 3932–3943.
- Zhan, S., Li, G., Na, J., and He, W. (2019b). Feedback non-causal model predictive control of wave energy converters. *Control Engineering Practice*, 85, 110–120.